Postprint of: Jasiński M., Yang L., Lamęcki A., Gomez-Garcia R., Mrozowski M., RF Multi-Functional Input-Reflectionless Dispersive-Delay Structure With Sharp-Rejection Filtering Using Channelization Techniques, IEEE TRANSACTIONS ON CIRCUITS AND SYSTEMS II-EXPRESS BRIEFS, Vol. 70, No 4 (2022), pp. 1410-1414, DOI: 10.1109/TCSII.2022.3228391

RF Multi-Functional Input-Reflectionless Dispersive-Delay Structure With Sharp-Rejection Filtering Using Channelization Techniques

Maciej Jasinski, *Graduate Student Member, IEEE*, Li Yang, *Member, IEEE*, Adam Lamecki, *Senior Member, IEEE*, Roberto Gómez-García, *Senior Member, IEEE*, and Michal Mrozowski, *Fellow, IEEE*

***Abstract*—A class of RF multi-functional input-reflectionless dispersive-delay structure (DDS) with linear-type in-band group-delay variation and sharp-rejection bandpass-filtering capability is reported. It exploits a two-branch-channelized/balanced-type circuit with similar low-order reflective DDS units inside its channels, which are connected through input/output 3-dB quadrature wideband couplers. The adopted DDS unit is based on a coupled-resonator network with a frequency-dependent cross-coupling. It introduces a pair of complex transmission zeros (TZs) to shape the intended in-band group-delay profile. Unequal transmission-line-based phase-shifting sections are also inserted at the outputs of both channels. In this manner, an input-absorptive behavior and selectivity enhancement with TZ generation are attained by means of transversal signal-interference techniques at the overall input and output nodes, respectively. Moreover, as the transfer-function phase term of the interference action in transmission is linear with frequency, the total group-delay pattern is defined by the DDS unit of the channels. As practical validation, a 1.5-GHz proof-of-concept microstrip prototype is constructed and tested.**

***Index Terms*—Absorptive filter, bandpass filter, channelized filter, coupling-matrix synthesis, dispersive-delay structure (DDS), frequency-dependent coupling, group delay, microstrip filter, planar filter, reflectionless filter, RF-analog-signal processing, signal interference, transmission zero (TZ), transversal filter.**

I. Introduction

IN ORDER to handle the ever-growing number of users, RF wireless systems have to constantly improve their performance in more-efficient realizations. One of the emerging trends to enable such evolution is the design of RF devices that can perform several functionalities simultaneously. This approach leads to more-compact RF structures that can fully replace cascades of various mono-functional RF components in traditional RF-front-end chains. Within this background, an increasing interest is lately being detected on multi-functional RF filtering devices, such as multi-mode switchable filters [1], [2], co-designed filtering power dividers [3]–[5], differentially-fed filtering antennas [6], and ultra-wideband bandpass filters with embedded adaptive notches [7], among many others.

It is well known that most of conventional RF bandpass filtering devices allow signal transmission within the band of interest while inhibiting it outside their passband by reflecting the unwanted frequencies. However, these out-of-band RF power reflections can severely interfere the operation of preceding RF active stages, such as amplifiers and mixers, by inducing them to work in non-linear regime or by generating additional spurious terms. This may potential lead to the malfunctioning of the entire RF front-end chain. As a result, the incorporation of reflectionless behavior in bandpass filters by making them to be lossy within their stopband range is a desired feature. This has been accomplished in the past by means of different design strategies with their benefits and drawbacks, such as the employment of two-branch/balanced circuits [8], [9], lossy circuits with even/odd-mode sub-network compensation [10], [11], complementary-diplexer topologies [12]–[15], filters with lossy matching networks including dissipative stubs [16]–[18], and transistor-based active cells with absorptive features [19].

On the other hand, once the desired RF signal has been acquired after RF bandpass filtering, it is then processed to extract the information or to prepare it for further transmission. This can be carried out by means of digital-signal-processing blocks, although with some limitations. Firstly, the signal must be converted from the analog to the digital domain, which leads to some quality degradation. Secondly, the performance of analog-to-digital converters, as well as of digital-signal-processing devices, deteriorates at high frequencies. Thirdly, the digital approach is more energy-consuming and suffers from heat-dissipation issues, which hinders its use in modern low-power/energy-efficient/green RF transceivers. A suitable alternative in this scenario is RF-analog-signal processing, which can overcome all the aforementioned shortcomings [20].

RF-analog-signal processing has found a wide range of applications, especially in the last few years. Several types of RF-analog-signal processors have been reported in the technical literature, such as phase-equalization circuits [21], frequency-discrimination devices [22], time stretchers of the RF signal [23], and pulse-position modulators [24]. As their fundamental circuit elements, all these RF-analog-signal-processing systems are based on dispersive-delay structures (DDSs). They operate over the RF signal by introducing a specific delay to each spectral component. This operation can be realized by means of different approaches, such as chirped lines [25], surface-acoustic-wave (SAW) devices [26], Bragg-grating sections [27], magnetostatic-wave (MSW) circuits [28], composite right/left-handed (CRLH) transmission lines [29], cascaded C-sections [30], and coupled-resonator filters [31]–[33].

In this brief, an RF multi-functional input-reflectionless

This work was supported in part by the National Science Centre, Poland, under Grant UMO-2019/33/B/ST7/00889 and in part by the Spanish Ministry of Economy, Industry, and Competitiveness (State Research Agency) under Project PID2020-116983RB-I00.

M. Jasinski, A. Lamecki and M. Mrozowski are with the Faculty of Electronics, Telecommunications, and Informatics, Gdańsk University of Technology, 80-233 Gdansk, Poland (e-mail: maciej.jasinski@pg.edu.pl; adam.lamecki@ieee.org; m.mrozowski@ieee.org).

L. Yang and R. Gómez-García are with the Department of Signal Theory and Communications, Polytechnic School, University of Alcalá, 28871 Alcalá de Henares, Spain (e-mail: li.yang@uah.es; roberto.gomez.garcia@ieee.org).

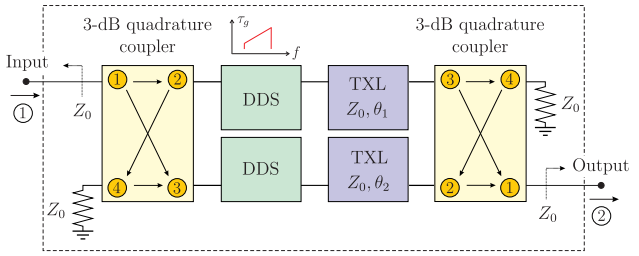

Fig. 1. Conceptual block diagram of the proposed RF input-reflectionless sharp-rejection filtering DDS (Ports of the coupler: 1-input; 2-direct; 3-coupled; 4-isolated; Z_0: reference impedance; θ_1 and θ_2: electrical lengths; τ_g: group delay; f: frequency; TXL: transmission line).

filtering DDS using a two-branch-channelized/balanced circuit is presented. This co-designed RF device exhibits following features: (i) bandpass filtering response, (ii) high selectivity owing to the presence of transmission zeros (TZs), (iii) in-band linear-type group-delay shape, and (iv) broad-band input-absorptive behavior. To the best of the author's knowledge, this is the first time all these functionalities are combined in the same RF component. Moreover, the group-delay characteristic and the selectivity-enhancement/input-reflectionless capabilities are designed separately, without affecting each to the other.

The rest of this brief is organized as follows: the circuit architecture and basic theoretical foundations of the proposed concept of RF input-reflectionless filtering DDS with TZs are detailed in Section II. For experimental-validation purposes, the simulated and measured results of a manufactured proof-of-concept microstrip prototype centered at 1.5 GHz are shown in Section III. Finally, a summary and the most relevant concluding remarks of this brief are provided in Section IV.

II. Theoretical Foundations

The conceptual circuit architecture of the proposed approach of RF multi-functional input-reflectionless sharp-rejection filtering DDS is presented in Fig. 1. As can be seen, it is inspired on the hybridization of balanced- and two-branch channelized topologies that have been separately applied in the past to absorptive and high-selectively bandpass filter design [9], [34]. The channels are made up of an identical low-order reflective DDS unit and a different transmission-line-based delay section at their outputs. In this manner, both channels exhibit the same amplitude transmission response—which is defined by the DDS unit—but distinct phase transmission responses due to the output phase-delay sections. The two channels are interconnected by means of input/output 3-dB quadrature couplers for 90°-offset RF-power-division/combination purposes.

By assuming that the 3-dB quadrature couplers are ideal, the analytical expressions for the overall input-power-reflection and transmission parameters in magnitude, $|S_{11}^T(f)|$ and $|S_{21}^T(f)|$, respectively, are as follows:

$$|S_{11}^T(f)| = 0 \qquad |S_{21}^T(f)| = |S_{21}^{\text{DDS}}(f)||S_{21}^{\Delta\theta}(f)|, \tag{1}$$

$$S_{21}^{\Delta\theta}(f) = \frac{e^{-j\theta_1(f)}}{2}\left(1 + e^{-j\Delta\theta(f)}\right) \tag{2}$$

where $\Delta\theta(f) = \theta_2(f) - \theta_1(f)$ and $S_{21}^{\text{DDS}}(f)$ and $S_{21}^{\Delta\theta}(f)$ are the power transmission parameters of the low-order DDS unit and the transversal signal-interference term, respectively. The formula of the overall group-delay $\tau_g^T(f)$ is given by

$$\tau_g^T(f) = \tau_g^{\text{DDS}}(f) + \tau_g^{\Delta\theta} \tag{3}$$

where $\tau_g^{\text{DDS}}(f)$ is the group-delay response of the DDS unit and $\tau_g^{\Delta\theta}$ is a constant-frequency group-delay term associated to the transversal signal-interference action in transmission. Therefore, from (1)–(3), the RF operational principles of the overall circuit in Fig. 1 can be summarized as follows:

- In reflection, the RF-power echoes coming from the reflective low-order DDS units in their out-of-band regions inter-cancel out at the overall input port—as they appear with the same magnitude but with opposite phases. Hence, any out-of-band reflected RF power is dissipated in the resistor loading the isolated port of the input coupler. Thus, an input-reflectionless behavior is obtained.
- In transmission, the low-order filtering response of the DDS units is transformed into a sharp-rejection filtering profile. This is due to the transversal signal-interference phenomenon inherent to the total circuit owing to the action of the transmission-line-based phase-delay sections. Furthermore, the overall group-delay shape is fully determined by the one designed for the low-order DDS unit.

Further explanation about the referred RF operational foundations of the devised input-reflectionless filtering DDS through the description of its main building blocks is provided below.

A. Low-Order DDS Units

For the design of the low-order DDS units that are embedded in both branches of the RF multi-functional circuit in Fig. 1, the coupled-resonator approach that was introduced in [33] is employed. In particular, as illustrated in the coupling-routing diagram provided in Fig. 2(a), a third-order circuit network in the form of a triplet with a frequency-dependent cross coupling is utilized. This frequency-variant cross coupling allows the generation of two complex TZs, which are essential for the shaping of the desired group-delay profile.

In the specific example that is presented in this work, an in-band group-delay profile that increases linearly with frequency was targeted in the synthesis process of the low-order DDS unit. Its center frequency is chosen as $f_0 = 1.5$ GHz, whereas the bandwidth for which the group delay is linear is 80 MHz. The maximum in-band group-delay variation is 4.18 ns, which gives rise to a slope coefficient equal to 52.28 ns/GHz. The theoretical input-power-reflection, transmission, and group-delay responses of the synthesized third-order DDS unit—in-band detail—are represented in Fig. 2(b). The values of the self-resonant and coupling coefficients in the lowpass domain for this design example are listed in the caption of this figure. As demonstrated, the intended linear-type group-delay shape is realized, along with a third-order reflective-type filtering action with in-band input-power-matching levels above 20 dB.

B. Transmission-Line-Based Phase-Delay Sections

The main purpose of the transmission-line-based phase-delay sections with electrical lengths θ_1 and θ_2 and characteristic impedance Z_0 is to increase the selectivity in the overall filtering response through frequency-dependent transversal signal-interference phenomena. This is revealed by (1) and (2),

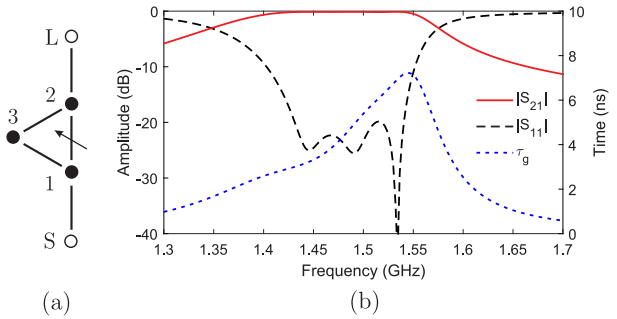

Fig. 2. Synthesized DDS unit based on a third-order coupled-resonator network with frequency-dependent cross coupling. (a) Coupling-routing diagram (white circles: source (S) and load (L); black circles: resonating nodes; continuous lines: constant couplings; continuous line with arrow: frequency-dependent coupling). (b) Theoretical power-transmission ($|S_{21}|$), input-reflection ($|S_{11}|$), and group-delay (τ_g) responses ($M_{11} = -0.236$, $M_{22} = 0.332$, $M_{33} = -0.214$, $M_{S1} = 1.251$, $M_{12} = 1.073$, $M_{23} = 1.149$, $M_{3L} = 1.422$, and $M_{13} = -0.432\Omega + 0.558$; $\Omega = (1/\Delta)(f/f_0 - f_0/f)$: normalized frequency; $f_0 = 1.5$ GHz and $\Delta = 0.0533$).

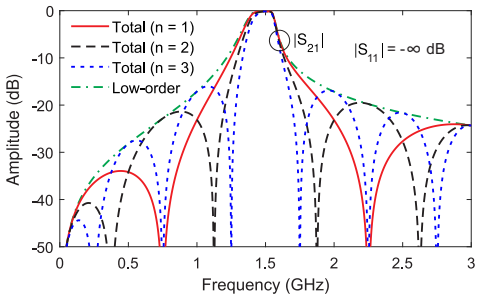

Fig. 3. Theoretical power transmission response ($|S_{21}|$) of the RF input-reflectionless sharp-rejection filtering DDS in Fig. 1—along with the one of its constituent third-order DDS unit in Fig. 2—for different values of n.

which shows that the overall transfer function in magnitude is given by the product of the one of the low-order DDS unit and a transversal signal-interference term in transmission mode. Specifically, constructive signal combination at the low-order DDS center frequency f_0 and destructive signal interactions to generate TZs at its out-of-band region must be produced. By assuming that $\theta_2(f_0) > \theta_1(f_0)$ without loss of generality, this is accomplished if the design equation below is satisfied:

$$\Delta\theta(f_0) = 2n\pi, \quad n \in \mathbb{N}. \tag{4}$$

Under this design condition, a total of $2n$ TZs are generated in the frequency range $[0, 2f_0]$. The formulas of the closest-to-f_0 lower and upper TZ frequencies, f_{zl} and f_{zu}, are

$$f_{zl} = \left(\frac{2n-1}{2n}\right) f_0 \qquad f_{zu} = \left(\frac{2n+1}{2n}\right) f_0, \tag{5}$$

so that the spacing between them is $\Delta f_z = f_{zu} - f_{zl} = f_0/n$. Thus, as n is increased, a higher number of out-of-band TZs and sharper cut-off slopes are obtained at the expense of a larger different between the lengths of the transmission-line segments—i.e., higher size and loss in a practical realization. This is corroborated by Fig. 3, which shows the theoretical power transmission response of the overall input-reflectionless sharp-rejection filtering DDS in Fig. 1—along with the one of its building third-order DDS unit for comparison purposes—for the DDS design example in Fig. 2 and several values of n.

Finally, as a key feature of the two-branch channelized-circuit architecture in Fig. 1, it should be remarked upon that the previously-referred increase of selectivity in the overall transfer function through multi-TZ creation is carried out without any effect on the overall group-delay shape. Indeed, as expressed in (3), the transversal signal-interference action in transmission only adds a constant-frequency factor in the overall group-delay response, whose pattern comes determined by the one designed for the low-order DDS unit. Specifically, under the design condition in (5), it can be demonstrated that such constant-frequency group-delay term is as follows:

$$\tau_g^{\Delta\theta} = -\frac{1}{2\pi}\frac{d\left(\angle S_{21}^T(f)\right)}{df} = \frac{1}{2f_0}\left(\frac{\theta_1(f_0)}{\pi} + n\right). \tag{6}$$

From the previous description, it is revealed that the design procedure to achieve the different performance features in the engineered RF multi-functional input-reflectionless sharp-rejection filtering DDS can be decorrelated, as follows:

1) Intended overall group-delay profile with the synthesis of the low-order DDS units in the branches.
2) Increase of the overall filtering selectivity through out-of-band multi-TZ creation with the design of the transmission-line-based phase-delay sections, where Δf_z must be larger than the low-order DDS passband width.
3) Input-absorptive behavior obtained intrinsically from the two-branch balanced-circuit architecture by means of the action of the 3-dB quadrature coupler at the input access.

III. Experimental Results

In order to demonstrate the experimental viability of the engineered approach of RF multi-functional input-reflectionless sharp-rejection-filtering DDS, a proof-of-concept prototype in microstrip technology has been manufactured and characterized. It corresponds to the design example illustrated in Fig. 3 of Section II for $n = 3$—i.e., $\Delta\theta(f_0) = 1080^o$ with $f_0 = 1.5$ GHz— and a reference-impedance level $Z_0 = 50\ \Omega$. For circuit fabrication, a Rogers' laminate RO4003 substrate with the following parameters was used: dielectric constant $\varepsilon_r = 3.55$, dielectric thickness $h = 0.508$ mm, dielectric loss tangent $\tan(\delta_D) = 0.0027$, and metal thickness $t = 17.4\ \mu$m. The simulations and optimization processes were carried out with the electromagnetic (EM) software package Ansys HFSS, whereas the measurements in terms of S-parameters were performed with an Agilent E8361A vector network analyzer.

In the DDS units of each channel, which consist of a third-order coupled-resonator network with a frequency-dependent coupling, the resonators were implemented as open-ended half-wavelength-at-1.5-GHz transmission-line segments. The dispersive coupling that is responsible for creating the two complex TZs, which are needed to shape the intended phase response, was also realized as an open-ended stub [33], [35].

Regarding the input/output 3-dB quadrature couplers, a three-stage version of the coupled-line coupler reported in [36] was utilized. It allows a compact physical realization while enabling a wide-band behavior in terms of 3-dB splitting factor and 90^o phase offset between output ports, which is essential to enlarge the input-reflectionless range of the overall RF device.

The layout—with indication of dimensions in mm—and photopragh of the manufactured microstrip prototype of input-reflectionless channelized filtering DDS are depicted in Fig. 4.

TABLE I
PERFORMANCE COMPARISON WITH OTHER PRIOR-ART DDS DEVICES

	Technology	GD profile	Frequency range (GHz)	$\Delta\tau$ (ns)	In-band IL (dB)	Asymmetry	TZs	Reflectionless
[23]	Microstrip	Linear	4–6	3.204	5	✓	×	×
[31]	Microstrip	Linear	2.4–2.6	7	3.75	✓	×	×
[32]	Waveguide	Linear	9.9–10.1	1.6	0.9	×	×	×
[33]	Waveguide	Linear	9.833–10.068	2.24	0.88	✓	×	×
[33]	Microstrip	Linear	19.355–2.065	0.61	1.22	✓	×	×
[33]	Microstrip	Stepped	1.905–2.095	1.08	1.69	✓	×	×
T.W.	Microstrip	Linear	1.401–1.479	3.8	5.76	✓	✓	✓ (input)

T.W.: this work; GD: group delay; IL: insertion loss; TZs: transmission zeros.

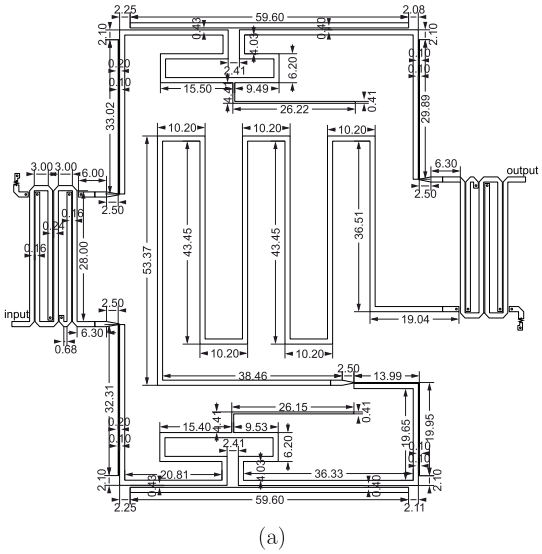

(a)

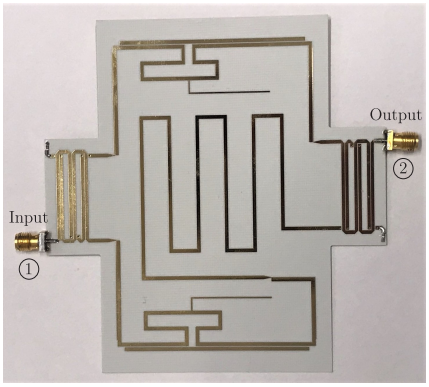

(b)

Fig. 4. Manufactured microstrip prototype of input-reflectionless channelized filtering DDS. (a) Layout (dimensions in mm). (b) Photograph.

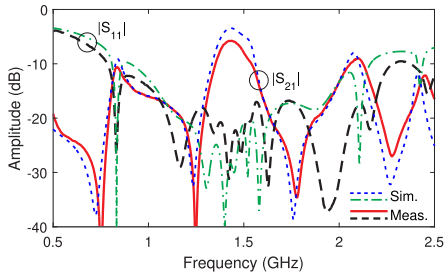

(a)

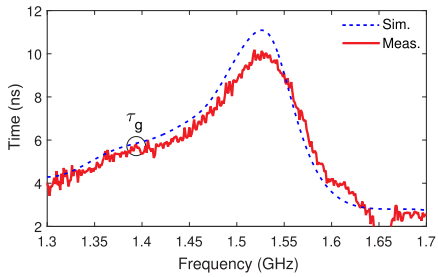

(b)

Fig. 5. EM-simulated and measured power-transmission ($|S_{21}|$), input-reflection ($|S_{11}|$), and in-band group-delay (τ_g) responses of the manufactured microstrip prototype of input-reflectionless channelized filtering DDS. (a) $|S_{21}|$ and $|S_{11}|$. (b) τ_g.

If necessary, further circuit-size reduction levels can be achieved by using fractal geometries or stub-loading techniques in the delay lines to make them electrically shorter, as respectively demonstrated in [37] and [38] for other transmission-line-based passive devices. Its EM-simulated and measured power-transmission, input-reflection, and in-band group-delay responses are compared in Fig. 5. As can be seen, apart from some additional loss in the experiment due to the different loss mechanisms of the circuit, a reasonable agreement between simulations and measurements is obtained, hence verifying the devised concept of multi-functional input-absorptive filtering DDS. Note that higher in-band insertion-loss levels are obtained in the upper region of the passband, which is a logical result as the in-band group delay increases linearly with frequency. The main measured performance metrics of the developed microstrip circuit of input-reflectionless filtering DDS are as follows: center frequency of 1.44 GHz, bandwidth equal to 78 MHz or 5.4% in relative terms—referred to the region in which the group delay is linear—, maximum in-band group-delay variation of 3.8 ns—i.e., group-delay slope coefficient of 48.72 ns/GHz—, minimum in-band power-insertion-loss level of 5.76 dB, and minimum in-band input-power-matching level equal to 20.8 dB. The measured 10-dB-referred input-reflectionless range is 0.783–2.278 GHz—i.e., 2.91:1 ratio. Besides, multiple TZs are created with those that are adjacent to the passband being located at 1.247 GHz and 1.78 GHz. A performance comparison of this DDS device with other prior-art DDS components is given in Table I. Note finally that, if needed by the intended application and like in its two-branch channelized filter precursor in [34], amplifier stages can be incorporated in the two branches of the input-reflectionless filtering phase-shifter circuit to compensate its relatively-high in-band insertion-loss levels.

IV. CONCLUSION

A type of co-designed RF circuit that simultaneously performs the DDS, sharp-rejection bandpass filtering, and input-reflectionless functionalities has been presented. It consists of

a channelized topology with identical low-order DDS units and different output-phase-delay sections at its two branches. The overall group-delay profile is determined by the one of the DDS unit, which increases linearly with frequency. Separately, the RF-input-absorption and selectivity-enhancement capabilities are realized through transversal signal-interference effects in reflection and transmission modes. The design foundations of the engineered input-reflectionless filtering DDS approach have been described. Furthermore, a demonstrative microstrip prototype centered at 1.5 GHz has been built and tested, showing a close agreement between simulations and measurements.

REFERENCES

[1] W. Feng, Y. Shang, W. Che, R. Gómez-García, and Q. Xue, "Multifunctional reconfigurable filter using transversal signal-interaction concepts," *IEEE Microw. Wireless Compon. Lett.*, vol. 27, no. 11, pp. 980–982, Nov. 2017.

[2] K. Zhao and D. Psychogiou, "Single-to-multi-band reconfigurable acoustic-wave-lumped-resonator bandpass filters," *IEEE Trans. Circuits Syst. II, Exp. Briefs*, vol. 69, no. 4, pp. 2066–2070, Apr. 2022.

[3] C. Zhu, J. Xu, W. Kang, and W. Wu, "Microstrip multifunctional reconfigurable wideband filtering power divider with tunable center frequency, bandwidth, and power division," *IEEE Trans. Microw. Theory Techn.*, vol. 66, no. 6, pp. 2800–2813, Jun. 2018.

[4] R. Gómez-García, J.-M. Muñoz-Ferreras, and D. Psychogiou, "RF reflectionless filtering power dividers," *IEEE Trans. Circuits Syst. II, Exp. Briefs*, vol. 66, no. 6, pp. 933–937, Jun. 2019.

[5] W. Feng, X. Ma, R. Gómez-García, Y. Shi, W. Che, and Q. Xue, "Multifunctional balanced-to-unbalanced filtering power dividers with extended upper stopband," *IEEE Trans. Circuits Syst. II, Exp. Briefs*, vol. 67, no. 7, pp. 1154–1158, Jul. 2019.

[6] H. Tian, Z. Chen, L. Chang, R. Wang, H. Wang, H. Liu, C. Du, D. Zhou, and Z. Wa, "Differentially fed duplex filtering dielectric resonator antenna with high isolation and CM suppression," *IEEE Trans. Circuits Syst. II, Exp. Briefs*, vol. 69, no. 3, pp. 979–983, Mar. 2022.

[7] D. Psychogiou, R. Gómez-García, and D. Peroulis, "RF wide-band bandpass filter with dynamic in-band multi-interference suppression capability," *IEEE Trans. Circuits Syst. II, Exp. Briefs*, vol. 65, no. 7, pp. 898–902, Jul. 2018.

[8] A. C. Guyette, I. C. Hunter, and R. D. Pollard, "Design of absorptive microwave filters using allpass networks in a parallel-cascade configuration," in *Proc. IEEE MTT-S Int. Microw. Symp.*, Boston, MA, USA, Jul. 2009, pp. 733–736.

[9] M. Fan, K. Song, L. Yang, and R. Gómez-García, "Frequency-tunable constant-absolute-bandwidth single-/dual-passband filters and diplexers with all-port-reflectionless behavior," *IEEE Trans. Microw. Theory Techn.*, vol. 69, no. 2, pp. 1365–1377, Feb. 2021.

[10] M. A. Morgan and T. A. Boyd, "Theoretical and experimental study of a new class of reflectionless filter," *IEEE Trans. Microw. Theory Techn.*, vol. 59, no. 5, pp. 1214–1221, Apr. 2011.

[11] M. A. Morgan, W. M. Groves, and T. A. Boyd, "Reflectionless filter topologies supporting arbitrary low-pass ladder prototypes," *IEEE Trans. Circuits Syst. I, Reg. Papers*, vol. 66, no. 2, pp. 594–604, Feb. 2019.

[12] R. Gómez-García, J.-M. Muñoz-Ferreras, and D. Psychogiou, "High-order input-reflectionless bandpass/bandstop filters and multiplexers," *IEEE Trans. Microw. Theory Techn.*, vol. 67, no. 9, p. 3683–3695, Sep. 2019.

[13] C. Luo, S.-W. Wong, J.-Y. Lin, Y. Yang, Y. Li, X.-Z. Yu, L.-P. Peng, Z.-H. Tu, and L. Zhu, "Quasi-reflectionless microstrip bandpass filters using bandstop filter for out-of-band improvement," *IEEE Trans. Circuits Syst. II, Exp. Briefs*, vol. 67, no. 10, pp. 1849–1853, Oct. 2020.

[14] M. Fan, K. Song, L. Yang, and R. Gómez-García, "Frequency-reconfigurable input-reflectionless bandpass filter and filtering power divider with constant absolute bandwidth," *IEEE Trans. Circuits Syst. II, Exp. Briefs*, vol. 68, no. 7, pp. 2424–2428, Jul. 2021.

[15] J. Lee and J. Lee, "Transmission-line bandpass filter structures with infinite reflectionless range," *IEEE Trans. Circuits Syst. I, Reg. Papers*, vol. 69, no. 6, pp. 2387–2398, Jun. 2022.

[16] T.-H. Lee, B. Lee, and J. Lee, "First-order reflectionless lumped-element lowpass filter (LPF) and bandpass filter (BPF) design," in *Proc. IEEE MTT-S Int. Microw. Symp.*, San Francisco, CA, USA, May. 2016, pp. 1–4.

[17] L. Yang, R. Gómez-García, J.-M. Muñoz-Ferreras, R. Zhang, D. Peroulis, and L. Zhu, "Multilayered reflectionless wideband bandpass filters with shunt/in-series resistively terminated microstrip lines," *IEEE Trans. Microw. Theory Techn.*, vol. 68, no. 3, pp. 877–893, Mar. 2020.

[18] Y. Zhang, Y. Wu, W. Wang, and J. Yan, "High-performance common- and differential-mode reflectionless balanced band-pass filter using coupled ring resonator," *IEEE Trans. Circuits Syst. II, Exp. Briefs*, vol. 69, no. 3, pp. 974–978, Mar. 2022.

[19] Q. Li, H. Tang, D. Tang, Z. Deng, and X. Luo, "Compact SIDGS filtering power divider with three-port 10-ghz reflectionless range," *IEEE Trans. Circuits Syst. II, Exp. Briefs*, vol. 69, no. 7, pp. 3129–3133, Jul. 2022.

[20] C. Caloz, S. Gupta, Q. Zhang, and B. Nikfal, "Analog signal processing: A possible alternative or complement to dominantly digital radio schemes," *IEEE Microw. Mag.*, vol. 14, no. 6, pp. 87–103, 2013.

[21] X. Zhao, S. Xiao, and Z. Jiang, "Asymmetric reflection-type all-pass equalizer," *IEEE Microw. Wireless Compon. Lett.*, vol. 29, no. 3, pp. 189–191, Mar. 2019.

[22] B. Nikfal, D. Badiere, M. Repeta, B. Deforge, S. Gupta, and C. Caloz, "Distortion-less real-time spectrum sniffing based on a stepped group-delay phaser," *IEEE Microw. Wireless Compon. Lett.*, vol. 22, pp. 601–603, 11 Nov. 2012.

[23] B. Nikfal, Q. Zhang, and C. Caloz, "Enhanced-SNR impulse radio transceiver based on phasers," *IEEE Microw. Wireless Compon. Lett.*, vol. 24, no. 11, pp. 778–780, Nov. 2014.

[24] H. V. Nguyen and C. Caloz, "CRLH delay line pulse position modulation transmitter," *IEEE Microw. Wireless Compon. Lett.*, vol. 18, no. 8, pp. 527–529, Aug. 2008.

[25] J. Schwartz, J. Azaña, and D. Plant, "Experimental demonstration of real-time spectrum analysis using dispersive microstrip," *IEEE Microw. Wireless Compon. Lett.*, vol. 16, no. 4, pp. 215–217, Apr. 2006.

[26] M. Lewis, "SAW and optical signal processing," in *Proc. IEEE Ultrasonics Symp.*, Rotterdam, Netherlands, Sep. 2005, pp. 800–809.

[27] B. E. A. Saleh and M. C. Teich, *Fundamentals of Photonics, 2nd ed.* Wiley-Interscience, 2007.

[28] W. Ishak, "Magnetostatic wave technology: A review," *Proc. IEEE*, vol. 76, no. 2, pp. 171–187, Feb. 1988.

[29] S. Gupta, S. Abielmona, and C. Caloz, "Microwave analog real-time spectrum analyzer (RTSA) based on the spectral–spatial decomposition property of leaky-wave structures," *IEEE Trans. Microw. Theory Techn.*, vol. 57, no. 12, pp. 2989–2999, Dec. 2009.

[30] H. V. Nguyen and C. Caloz, "Generalized coupled-mode approach of metamaterial coupled-line couplers: Coupling theory, phenomenological explanation, and experimental demonstration," *IEEE Trans. Microw. Theory Techn.*, vol. 55, no. 5, pp. 1029–1039, May 2007.

[31] W. Liao, Q. Zhang, Y. Chen, S. Wong, and C. Caloz, "Compact reflection-type phaser using quarter-wavelength transmission line resonators," *IEEE Microw. Wireless Compon. Lett.*, vol. 25, no. 6, pp. 391–393, Jun. 2015.

[32] Q. Zhang, D. L. Sounas, and C. Caloz, "Synthesis of cross-coupled reduced-order dispersive delay structures (DDSs) with arbitrary group delay and controlled magnitude," *IEEE Trans. Microw. Theory Techn.*, vol. 61, no. 3, pp. 1043–1052, Mar. 2013.

[33] M. Jasinski, M. Mul, A. Lamecki, R. Gómez-García, and M. Mrozowski, "Dispersive delay structures with asymmetric arbitrary group-delay response using coupled-resonator networks with frequency-variant couplings," *IEEE Trans. Microw. Theory Techn.*, vol. 70, no. 5, pp. 2599–2609, May 2022.

[34] R. Gómez-García, J. I. Alonso, and C. Briso-Rodríguez, "On the design of high-linear and low-noise two-branch channelized active bandpass filters," *IEEE Trans. Circuits Syst. II, Analog Digit. Signal Process.*, vol. 50, no. 10, pp. 695–704, Oct. 2003.

[35] L. Szydlowski, N. Leszczynska, and M. Mrozowski, "Generalized Chebyshev bandpass filters with frequency-dependent couplings based on stubs," *IEEE Trans. Microw. Theory Techn.*, vol. 61, no. 10, pp. 3601–3612, Oct. 2013.

[36] J.-H. Cho, H.-Y. Hwang, and S.-W. Yun, "A design of wideband 3-dB coupler with N-section microstrip tandem structure," *IEEE Microw. Wireless Compon. Lett.*, vol. 15, no. 2, pp. 113–115, Feb. 2005.

[37] H. Ghali and T. A. Moselhy, "Miniaturized fractal rat-race, branch-line, and coupled-line hybrids," *IEEE Trans. Microw. Theory Techn.*, vol. 52, no. 11, p. 2513–2520, Nov. 2004.

[38] M. L. Chuang, "Miniaturized ring coupler of arbitrary reduced size," *IEEE Microw. Wireless Compon. Lett.*, vol. 15, no. 1, pp. 16–18, Jan. 2005.